THE OFFICIAL MAGAZINE OF THE OCEANOGRAPHY SOCIETY

Oceanography

CITATION

Comfort, C.M., M.A. McManus, S.J. Clark, D.M. Karl, and C.E. Ostrander. 2015. Environmental properties of coastal waters in Mamala Bay, Oahu, Hawaii, at the future site of a seawater air conditioning outfall. *Oceanography* 28(2):230–239, http://dx.doi.org/10.5670/oceanog.2015.46.

DOI

http://dx.doi.org/10.5670/oceanog.2015.46

COPYRIGHT

This article has been published in *Oceanography*, Volume 28, Number 2, a quarterly journal of The Oceanography Society. Copyright 2015 by The Oceanography Society. All rights reserved.

USAGE

Permission is granted to copy this article for use in teaching and research. Republication, systematic reproduction, or collective redistribution of any portion of this article by photocopy machine, reposting, or other means is permitted only with the approval of The Oceanography Society. Send all correspondence to: info@tos.org or The Oceanography Society, PO Box 1931, Rockville, MD 20849-1931, USA.

DOWNLOADED FROM HTTP://WWW.TOS.ORG/OCEANOGRAPHY

Environmental Properties of Coastal Waters in Mamala Bay, Oahu, Hawaii, at the Future Site of a Seawater Air Conditioning Outfall

By Christina M. Comfort, Margaret A. McManus, S. Jeanette Clark, David M. Karl, and Chris E. Ostrander





ABSTRACT. Shifting to renewable energy is an important global challenge, and there are many technologies available to help reduce carbon dioxide emissions. Seawater air conditioning (SWAC) is a renewable ocean thermal energy technology that will soon be implemented in Honolulu, Hawaii, on the island of Oahu. The SWAC system will operate by using cool water from 500 m depth in a heat exchange system and then will release this nutrient-rich water back into the ocean at a shallower depth of 100–140 m. The introduction of a plume of warmed (but still relatively cool) deep seawater has unknown impacts on the tropical marine environment. Possible impacts include increases in primary production, changes in water chemistry and turbidity, and changes in the local food web. We used moored instruments and shipboard profiling to describe oceanographic parameters at the future SWAC effluent site. Parameters varied with the M2 internal tide, and denser water was correlated with higher nitrate, lower oxygen, and lower chlorophyll *a* (correlation coefficients 0.55, –0.58, and –0.75, respectively). The nitrate concentrations in the plume will be >30.0 µmol kg^{-1}, while ambient concentrations range from <2.0–9.8 µmol kg^{-1}. Irradiance levels at the effluent depth are sufficient to support net photosynthesis, and the effluent's location in the pycnocline could lead to rapid horizontal advection of the plume and expansion of the spatial scale of impacts. These baseline data provide an understanding of pre-impact conditions at the future SWAC site and will enable a more accurate environmental assessment. A comprehensive and well-resolved environmental monitoring effort during SWAC operation will be necessary to quantify and understand these impacts.

INTRODUCTION

In the face of rising oil costs and greenhouse gas-induced climate change, renewable energy technologies are gaining traction in the global economy (Arent et al., 2011). Sources such as solar, wind, wave, and ocean thermal energy help to move electricity generation away from carbon-based fuels that drive anthropogenic climate change. Each renewable energy technology has environmental benefits and, conversely, unique environmental impacts that must be considered to understand the overall impact of these technologies on the local and global ecosystem (Pelc and Fujita, 2002; Gill, 2005; Boehlert and Gill, 2010; Comfort and Vega, 2011).

Seawater air conditioning (SWAC) and ocean thermal energy conversion (OTEC) are technologies that propose using cold seawater for energy. OTEC uses the thermal differential between warm surface seawater and cold deep seawater to generate electricity; SWAC uses cold seawater in a heat exchange system to air condition buildings. The potential environmental impacts of OTEC are discussed in the literature (e.g., Myers et al., 1986; Harrison, 1987; Boehlert and Gill, 2010; Comfort and Vega, 2011), but few studies have focused on the environmental impacts of SWAC, especially in tropical environments. However, the two technologies share some fundamental similarities. Both systems rely on cold ocean water, which in the tropics must be extracted from depth, and both return this water to shallower depths with similar potential impacts.

Specifically, SWAC pumps cold seawater to a station where it is used to cool a closed freshwater loop (War, 2011). The warmed seawater is released back into the ocean. The cooled freshwater interfaces with buildings' existing air conditioning systems in place of a traditional coolant, and can thereby provide renewably sourced air conditioning to a city district (War, 2011; Figure 1). SWAC technology has been implemented at the district scale in several temperate cities, including Amsterdam, Stockholm, and Vancouver, where cold water can be sourced from the surface ocean. Several deepwater SWAC systems operate at the individual building scale, including at a hotel in Tahiti and in administrative buildings at the Natural Energy Laboratory of Hawaii Authority campus (http://nelha.hawaii.gov/energy-portfolio; http://www.makai.com/pipelines/ac-pipelines/#case). However, no district-scale SWAC systems currently operates in a tropical ecosystem.

Honolulu Seawater Air Conditioning, LLC, plans to build the first tropical district-scale SWAC system. The system is designed to serve the downtown business district of Honolulu, HI, with 25,000 tons (12.5 million square ft) of centralized air conditioning (Honolulu Seawater Air Conditioning [SWAC], LLC, 2014), and construction is planned for late 2015 (Frederic Berg, Honolulu SWAC, *pers. comm.,* May 29, 2014). The system will deliver 167 m^3 min^{-1} of 7.2–10°C ocean water from 500 m depth to a land-based heat exchanger, warm the water by 6–7°C, and then release the warmed effluent via a 20-port diffuser at a depth of 100–140 m along the seafloor (the deepest depth economically feasible for the company). The environmental benefits of this system include projected reductions in oil use by 178,000 barrels per year, in freshwater use by 260 million gallons per year, and in CO_2 emissions by 84,000 tons per year (http://www.honoluluswac.com). Potential negative environmental impacts of the system are primarily related to the warmed deep seawater effluent. In a year, approximately 88×10^6 m^3 of seawater will move through the system into Mamala Bay (Honolulu SWAC, LLC, 2014), compared to an estimated water input of 100–300 $\times$ 10^6 m^3 yr^{-1} via streams and groundwater (Freeman, 1993; Stevenson et al., 1996). Wastewater treatment plants generate about 150×10^6 m^3 yr^{-1} of point source input (Stevenson et al., 1996; Laws et al., 1999). The proposed SWAC system would result in a 20–35% increase in water input to the bay, a significant alteration that necessitates a comprehensive environmental monitoring program.

Furthermore, deep seawater has a fundamentally different composition than shallow seawater in the stratified subtropical ocean near Hawaii. Water sourced from 500 m depth near Hawaii is relatively lower in temperature, higher in nutrients, lower in oxygen, and higher in dissolved inorganic carbon than photic zone

water (Hayward, 1987). The temperature of the deep seawater changes as it moves through the SWAC heat exchanger, affecting the solubility of dissolved gases and the fluid density. The artificial upwelling of this nutrient-rich water to the photic layer could cause an array of impacts, including increased primary production, changes in turbidity, increases in the partial pressures of carbon dioxide and nitrous oxide, alteration of the microbial composition in the photic layer, and changes in the local food web (NOAA, 1981; Myers et al., 1986).

The possibility of increased primary production is critically dependent on the density of the plume and the depth of release. If the isopycnal depth of the plume is above the compensation depth, primary production could increase due to the input of bioavailable, fixed inorganic nutrients (Laws et al., 2014). Preliminary mesocosm experiments found that adding nutrient supplements rich in both nitrate and phosphate generated the greatest phytoplankton production response, and the SWAC plume will indeed have elevated concentrations of these nutrients (Lilley et al., 2012). Additionally, the environmental impact of SWAC systems in Hawaii is of keen interest to the tourism industry and to the general public (Lilley et al., 2012).

Because the potential environmental impacts surrounding the operation of district-scale SWAC in Honolulu are unknown, we have identified a need to observe and quantify relevant oceanographic parameters at the site of the future effluent, both before and during operation. The present study focuses on oceanographic monitoring via moored instrumentation, vertical profiles, and water samples during the pre-impact period. We aim to describe the oceanography of the site by identifying dominant flow patterns and understanding the natural variability of parameters including temperature, salinity, nutrients, and oxygen so that future SWAC-related changes can be correctly identified and quantified. We also aim to gain a better understanding of the physical processes driving variability of these parameters.

METHODS

Study Site

Mamala Bay is an open embayment off the south shore of the island of Oahu, Hawaii. The bay spans 30 km from Barber's Point (21.29°N, 158.11°W) to Diamond Head (21.25°N, 157.81°W). The deployment location of a moored instrument package within the bay was selected to coincide with the future Honolulu SWAC, LLC, effluent pipe diffuser location (Honolulu SWAC, LLC, 2014; Figure 1). The diffuser will terminate in a small canyon outside Honolulu Harbor at approximately 21.280°N and 157.872°W and will release the effluent approximately 2.7 m above the seabed.

Data Collection

Two deployments of the moored instrument package are reported here, with deployment one from August 6–October 14, 2013 (70 days) and deployment two from November 8, 2013–February 20, 2014 (104 days). The mooring supported six instruments that measured current magnitude and direction, temperature, salinity, pressure, turbidity, fluorescence, and nitrate.

Shipboard conductivity-temperature-depth (CTD) casts were carried out at three locations: (1) a site near the top of the proposed diffuser, at ~100 m depth, (2) a site slightly downslope of the diffuser location at ~175 m depth, and (3) a site near the proposed seawater intake location at ~500 m depth (Figure 1b). The profiling CTD additionally hosted sensors measuring fluorescence, light transmission, nitrate, and oxygen. Bottle samples were taken at five to eight depths throughout the water column on each profile. Specifics of moored and profiling instruments and programming are provided in the online Supplementary Materials.

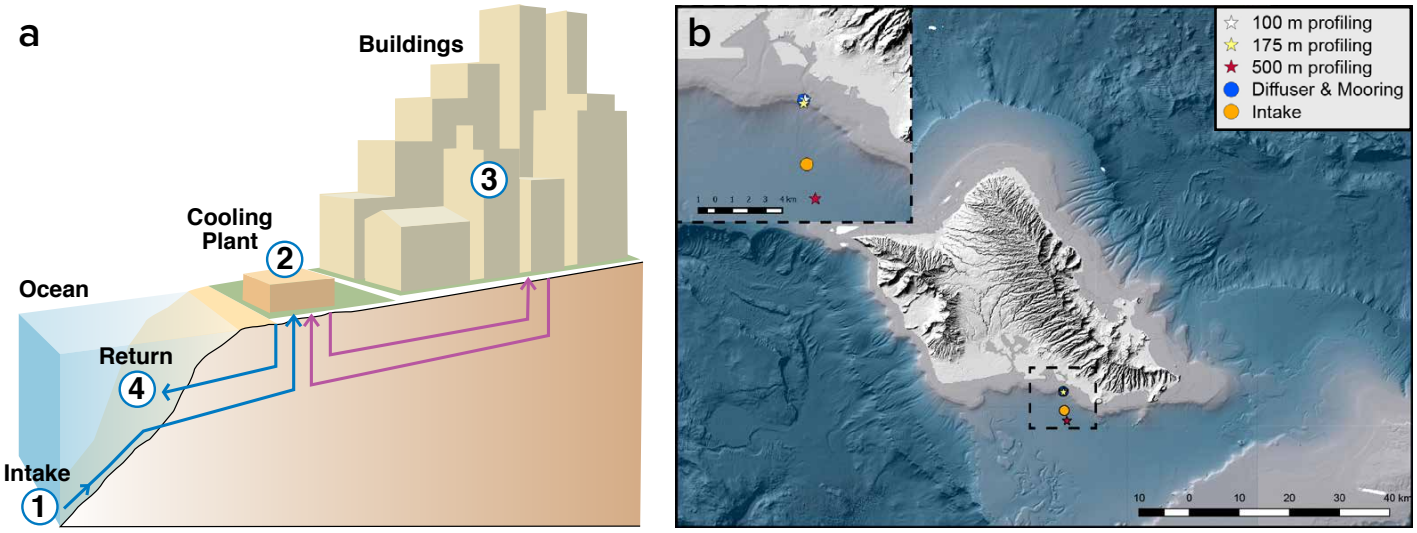


FIGURE 1. (a) Schematic of seawater air conditioning (SWAC). (1) Deep seawater intake pipe. (2) Heat exchange facility. (3) Cooled freshwater loop. (4) Seawater effluent pipe. *Figure modified from Karl (2014)* (b) Map of study site including the mooring and diffuser sites, the three shipboard profiling locations, and the deepwater intake site for Honolulu SWAC.

Data Analysis

Statistics and Spectral Analysis

The mean, standard deviation, minimum, and maximum of each measured variable were computed. Spectral analyses were carried out using the Fast Fourier Transform method (Cooley and Tukey, 1965; Brillinger, 2002). Current ellipses were calculated by finding the principal axes using Eigenvectors. Correlations between variables were found using a least-squares linear regression where appropriate, or when the relationship was nonlinear, the correlation was based on an appropriate nonlinear relationship found using the curve-fitting toolbox in MatLab.

Calculations

Light levels of 1% and 0.1% were determined for each profile by taking the natural log of the irradiance and computing the slope *m*, which equals the light attenuation coefficient *k*. The *k*-value was used to predict the depth of 1% and 0.1% light levels for each profile using the following formulas (Kirk, 1994):

(1) *Depth of 1% light level = ln(0.01)/k*

(2) *Depth of 0.1% light level = ln(0.001)/k*

The start of the pycnocline (the mixed layer depth) was calculated by locating the shallowest depth at which the density was 0.125 kg m^{-3} greater than the density at 10 dbar (Levitus, 1982). The thickness of the pycnocline was determined by creating cutoffs based on the rate of change in density over 1dbar bins. The density data were smoothed using a moving average filter with a span of 10 dbar to reduce noise. The steepest part of the pycnocline was defined as the mixed layer depth to the deepest depth where a rate of change of at least 0.025 kg m^{-3} per dbar was observed. The full pycnocline was defined as the mixed-layer depth to the deepest depth where the rate of change was at least 0.01 kg m^{-1} per dbar. Resulting pressures were converted to depth using an approximation of 1 dbar: 1.019716 m.

Plume Buoyancy Analysis

Gravity currents have been observed around the world, with the difference between cascading water and ambient water averaging 0.4 kg m^{-3} and as high as 2.0 kg m^{-3} (Ivanov et al., 2004). The SWAC effluent plume will be 2.0 kg m^{-3} denser than ambient water and can be treated as a gravity current from a fluid dynamics perspective. Baines (2001) describes the derivation of the momentum and mass balance for downslope flows into a stratified environment. To determine the relative importance of cross-shore currents on the effluent in comparison to the downslope density-driven flow, we used a momentum balance as described in Baines (2001), with the addition of a drag term representing the bed stress exerted by ambient flow on the plume.

RESULTS

Moored Sensors

Velocity

The acoustic Doppler current profiler (ADCP) reported east-west (u), north-south (v), and vertical (w) velocity components. Power spectral density analysis was done for the deepest bin (4.7–8.7 m above bottom) and for a mid-water bin (60.7–64.7 m above bottom). Spectral peaks were observed at M2 (12.4 h), M4 (6.1 h), and M6 (4.1 h) periodicities in both u and v directions (Table 1).

The isobath at the site of the mooring runs alongshore at ~295°, and therefore the perpendicular (cross-shore) direction is about 25°. Currents in the bottom layer were predominantly cross-

TABLE 1. Summary of power spectral density peaks for each variable observed in this study. Most parameters varied with the M2 tide, and signals at the K1 frequency were also found in several parameters.

Category	Parameter	Period (h)								
Measured Parameters	Temperature			6.21			12.45	24.03	25.83	
	High frequency temperature		4.10	6.19			12.51			
	Salinity			6.21			12.45	24.03		
	Depth			6.21			12.42	23.93	25.80	
	Fluorescence			6.10			12.45			
	Turbidity									
	Oxygen		4.13	6.21			12.40	24.08		
	Nitrate		4.10	6.30			12.83	24.40		
	Velocity (u, near bottom)		4.14	6.17			12.39			
	Velocity (v, near bottom)		4.14	6.20			12.39			
	Velocity (u, mid-water)		4.14	6.17			12.39			
	Velocity (v, mid-water)		4.14	6.20			12.39			
Weather	Wind					12.00		23.98		
Tides	K1 Tide							23.93		
	M2 Tide			6.21			12.42		24.84	
	Inertial									33.08

isobath (7.8° in the layer spanning 4.7–8.7 m above the bottom). In mid-water, flow was predominantly along-isobath (300.8° at 60.7–64.7 m above bottom) (Figure 2a). The major axis remained primarily cross shore from 4.7–32.7 m above bottom, and then was primarily alongshore from 32.7–116.7 m above bottom (Figure 2b). The transition from cross-shore-dominated to along-shore-dominated flow occurred primarily between 20.7–44.7 m above bottom, where 61.3° of major axis rotation occurred.

CTD and Auxiliary Sensors

A moored CTD with auxiliary optical sensors for oxygen, fluorescence, and light transmission collected data throughout both deployment periods (Table 2). In deployment one, water depth ranged from 144.16–144.96 m. In deployment two, depth ranged from 139.98–140.90 m. Tides in this region are mixed semidiurnal with maximum amplitude of approximately 0.9 m (Bondur et al., 2007).

The cross-shore currents described previously advected pulses of cooler, denser water upslope, which drove tidal variability in parameters associated with density. Higher fluorescence generally correlated with lower density (general power model curve fit; R = –0.75; R^2 = 0.57). Higher oxygen also tended to occur with lower density (general power model curve fit; R = –0.58; R^2 = 0.34). Salinity had a positive correlation with temperature (polynomial curve fit; R = 0.99; R^2 = 0.98) (Figure 3).

Spectral analyses of temperature, salinity, fluorescence, and oxygen revealed peaks at the M2 and M4 tidal constituent frequencies. Additionally, the M6 and K1 tidal frequencies were discernible in spectra of pressure, temperature, and oxygen data. Spectral analysis of turbidity did not produce any significant peaks (Table 1).

Long-term trends were mostly stable. Seasonal trends may exist, but a longer time series would be needed to discern them.

Nitrate

During deployment one, an optical nitrate sensor measured a mean nitrate concentration of 4.8 ± 0.9 µmol kg^{-1} (range <2.0–9.8 µmol kg^{-1}) at about 145 m depth. During deployment two, the mean nitrate concentration was 3.0 ± 0.8 µmol kg^{-1} (range <2.0–7.7 µmol kg^{-1}) at about 140 m depth. Prominent spectral peaks occurred at periods of 6.2 and 12.4 hours, corresponding to the M2 and M4 tidal frequencies. Higher water density tended to correspond to higher nitrate measurements (general power model curve fit; R = 0.55; R^2 = 0.30) (Figure 3d). Temperature and nitrate are inversely related (R = –0.77; R^2 = 0.59) and mirror each other on short time scales (Figure 4). While the tidal component is dominant, these variations show that shorter time scale processes are also present in this environment.

Anomalous nitrate trend in September: Generally, nitrate concentrations varied tidally with no overall increasing or decreasing trends (Figure 5). However, from September 12, 2013, 14:24 to September 14, 2013, 13:48, the minimum nitrate concentrations per tidal cycle increased from 3.1 µmol kg^{-1} to 5.2 µmol kg^{-1}, and then decreased back to 3.7 µmol kg^{-1} by September 15, 2013, 05:50. Nitrate concentrations remained above 4.9 µmol kg^{-1} for 24 hours starting on September 13, 2013, 16:48:00, the longest such observation in the time series.

Depth, density, temperature, wind speed, and wind direction were examined alongside the nitrate time series for the time period of the anomaly. Wind data were obtained from the Honolulu International Airport weather station records (http://www.uswx.com). No

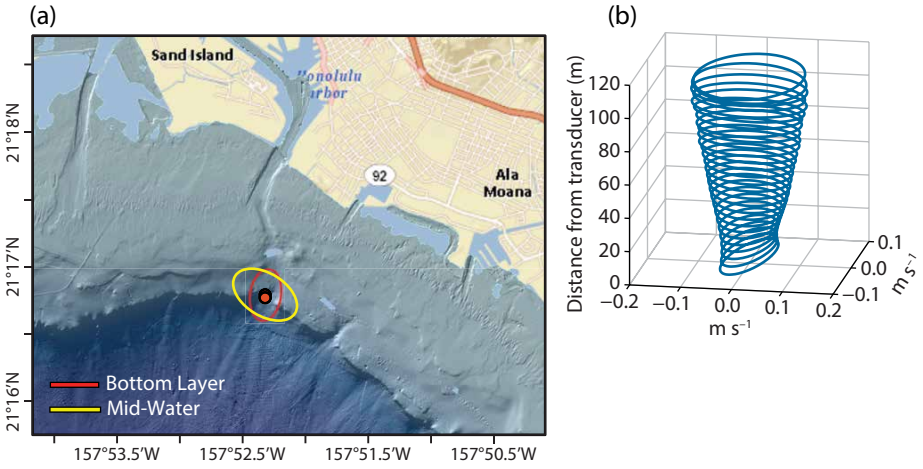


FIGURE 2. (a) Bottom layer and mid-water current ellipses plotted over bathymetry show bathymetric steering effects. (b) Current ellipses in 4 m bins throughout the water column. The dominant direction at the bottom of the water column is in the v direction, while in the mid and upper water column, the u direction is dominant.

TABLE 2. Mean, standard deviation, minimum, and maximum for parameters measured at the bottom mooring.

	Mean	SD	Minimum	Maximum
Temperature (°C)	20.59	1.09	16.00	25.08
Salinity (PSS)	35.18	0.10	34.60	35.40
Fluorescence (mg m^{-3})	0.19	0.09	0.03	1.18
Turbidity (NTU)	1.28	0.18	0.96	9.68
Oxygen (µmol kg^{-1})	197.90	2.52	189.53	209.36
Nitrate (Deploy 1, 145 m) (µmol kg^{-1})	4.7	1.1	<2.0	9.9
Nitrate (Deploy 2, 140 m) (µmol kg^{-1})	3.0	0.8	<2.0	7.7

obvious anomalies were observed in these properties during the time of the nitrate spike (Figure 5).

Shipboard Profiling

Intake Water Properties

The properties of the plume water were estimated using samples sourced from 480–520 m depth. The mean nitrate and phosphate concentrations were 33.2 ± 0.9 μmol kg^{-1} and 2.4 ± 0.1 μmol kg^{-1}, respectively. Mean oxygen concentration was 72.0 ± 6.4 μmol kg^{-1}. The SWAC flow rate of 88 × 10^6 m^3 yr^{-1} will result in a yearly input of 2.9 × 10^6 mol nitrate and 2.1 × 10^5 mol phosphate. These inputs will add to those of the existing wastewater treatment plants. Existing yearly inputs are 8.3 × 10^5 mol nitrate as part of a total dissolved nitrogen input of 1.7 × 10^8 mol, and 7.8 × 10^6 mol phosphate as part of a total dissolved phosphorus input of 8.2 × 10^6 mol (Laws et al., 1999).

Pycnocline

The mixed-layer depth was variable and ranged from 50.9–93.8 m in profiles taken at the 500 m site. At the two nearshore sites, the mixed layer was not always identifiable, but when it was, it ranged from 36.7–87.7 m water depth and was typically shallower than at the 500 m site on the same day. The thickness of the pycnocline could only be fully observed at the offshore site because the pycnocline intersected the benthos at the shallower sites. At the 500 m site, the thickness of the steepest part of the pycnocline was variable (0.025 kg m^{-3} change in density per dbar, mean thickness 82.7 ± 62.2 m). The total thickness of the pycnocline was 237.0 ± 41.5 m using a minimum of 0.01 kg m^{-3} change in density per dbar.

Chlorophyll Maximum

The chlorophyll maximum was consistently observed at the 175 m and 500 m water depth stations, and sometimes observed at the 100 m station. The mean depth of the chlorophyll maximum was 60.8 ± 13.81 m at the 100 m site, 64.6 ± 21.04 m at the 150 m site, and 92 ± 25.39 m at the 500 m site. The beginnings of the nutricline and oxycline were generally observed between 125 and 150 m at all three sites. The chlorophyll maximum was observed higher in the water column than the start of the oxycline and nutricline, but elevated fluorescence levels were found as deep as 200 m (Figure 6).

Photosynthetically Active Radiation

Adequate photosynthetically active radiation (PAR) is necessary for phytoplankton to maintain net primary production. In general, PAR decreases logarithmically with depth, and the rate of this decrease is used to determine the compensation depth, below which net primary production cannot occur. The mean 1% light level occurred at 100.3 ± 20.0 m, and the 0.1% light level at 150.5 ± 30.1 m (Figure 7).

Plume Buoyancy

Assuming low friction between the upper interface of the plume and the surrounding water, and assuming that the pressure gradient term is small, the buoyancy force, plume drag force, and background drag force are on the orders of 10^{-2}, 10^{-5}, and 10^{-7}, respectively. Based on these values, it is clear that the buoyancy force will be dominant and the background drag force will be negligible in comparison. Although mixing from the diffuser has not been specifically considered here, the buoyancy term is large enough that, even with mixing due to entrainment of

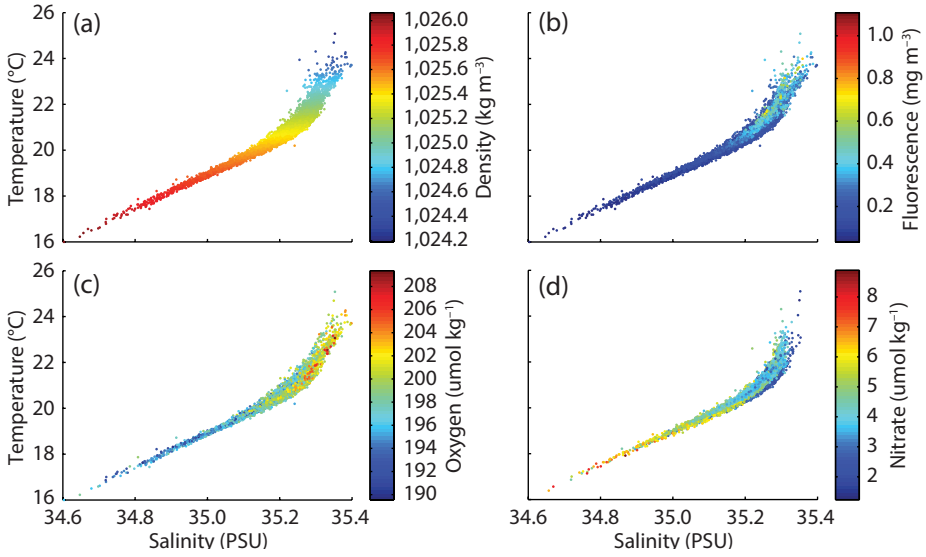


FIGURE 3. Temperature-salinity plots produced from moored data overlain with (a) density, (b) fluorescence, (c) oxygen, and (d) nitrate. Oxygen and fluorescence have a generally positive relationship with density, while nitrate is generally negative. The variability observed here is primarily due to internal tides.

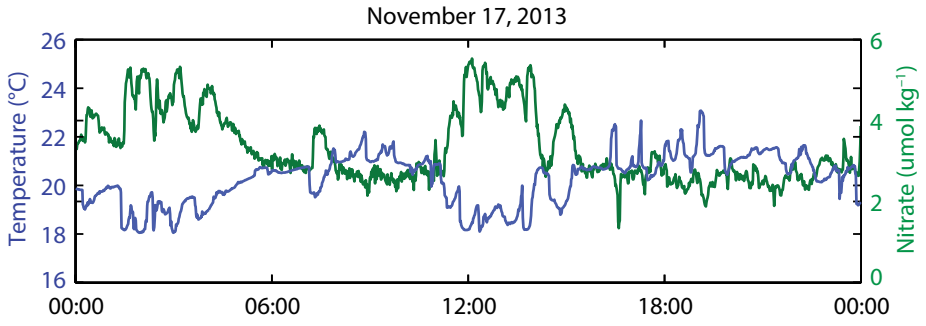


FIGURE 4. Nitrate and temperature measured at one-minute intervals on November 17, 2013. Temperature and nitrate have an inverse relationship, even at short time scales.

surrounding water and shear-induced turbulence, the overall tendency of the plume will be to sink, and onshore advection of the plume will most likely be minimal.

DISCUSSION

Environment at the Proposed SWAC Site

Water Column Structure

The oceanographic properties measured during shipboard profiling suggest a typical tropical oligotrophic environment in this area of Mamala Bay. Low surface nutrients and chlorophyll *a*, a deep chlorophyll maximum in the 20–90 m range, and higher nutrient levels below the thermocline were observed. The mixed layer was shallower at the 100 m and 150 m stations compared to the 500 m station. The island shadows nearshore stations from east-northeasterly trade winds, while the 500 m station is more exposed (Figure 1). At all three stations, the 1% to 0.1% light levels were observed between about 100 and 150 m average depth. The compensation depth has recently been estimated to occur at 0.11% of surface light levels in the Hawaiian ocean (Laws et al., 2014). The availability of light in the 100–140 m depth range indicates that the high-nutrient effluent from the SWAC diffuser pipe may enhance primary production in this zone.

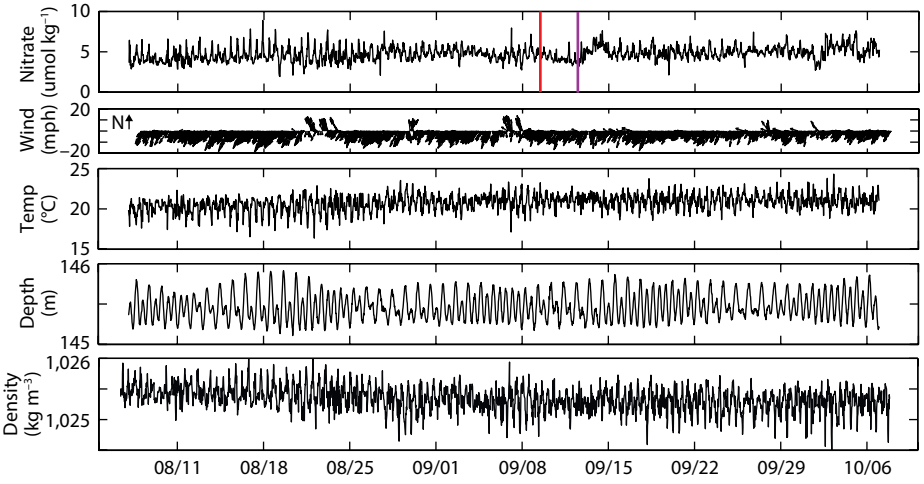


FIGURE 5. Nitrate time series with wind, temperature, tide, and density. An anomalous increasing trend in nitrate alone was observed in mid-September (purple). A molasses spill occurred 4.42 km away in Honolulu harbor on September 9, 2013 (red). If the molasses spill caused the observed spike in nitrate, the flow would have traveled a reasonable 1.58 cm s^{-1} downslope. The detection of this event provides confidence in the ability to detect anthropogenic inputs of nutrients at our mooring site.

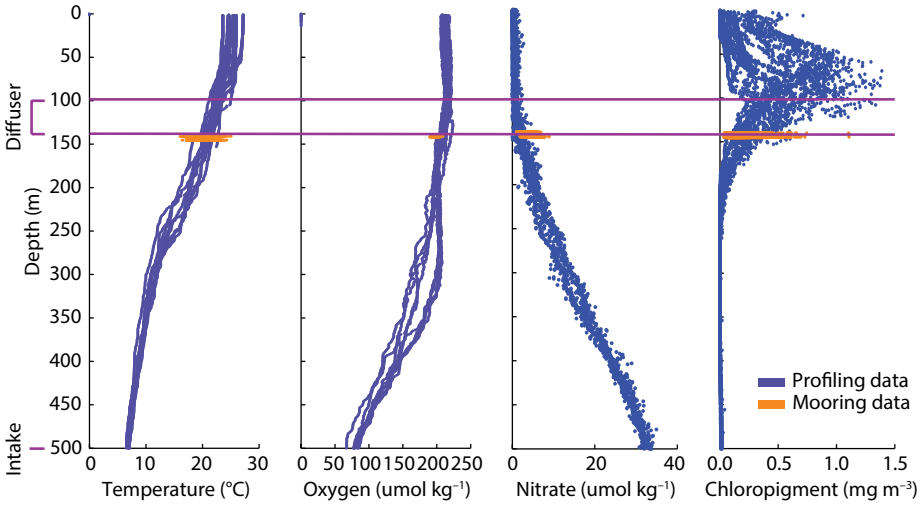


FIGURE 6. Depth profiles of temperature, oxygen, nitrate, and chloropigment with the depths of SWAC intake and diffuser. The high levels of nutrients in deep intake water could cause enhanced primary production if released above the phytoplankton compensation depth.

Internal Tides, Bathymetric Steering, and Parameter Variability

Surface and internal tides affect coastal waters in Mamala Bay (Merrifield et al., 2001; Alford et al., 2006), and the dominant tidal variability in parameters observed here reflect that. The observed M2/M4 variability (in temperature, nitrate, oxygen, and density) and the dominant cross-shore flow observed near bottom are consistent with internal tidal forcing of water through the cross-isobath channel where the mooring was situated (Figure 1 inset). The internal tides observed in Mamala Bay are generated at the flanks of ridges at the southeastern corner of the island, Makapuu Point (Martini et al., 2007), and additionally are influenced by internal tides generated at Kaena Ridge at the northwestern corner of the island (Eich et al., 2004). Vertical displacements up to 200 m have been observed near the Kaena Ridge location (Nash et al., 2006). The tidal variability in temperature and other parameters observed in this study is comparable to values in the literature (Petrenko et al., 2000; Eich et al., 2004; Bondur et al., 2007), and corresponds to vertical displacements of isotherms of 80–90 m (Figure 5). The bathymetric steering of currents in the channel may amplify this variability near the benthos.

Several other studies in Hawaii and in the Florida Keys have identified cold pulses on shallow slopes near the bottom (e.g., Leichter et al., 2003; Sevadjian et al., 2012). On Oahu, M2-frequency cold pulses have been previously identified in Mamala Bay at a depth of 40 m, and cold pulses throughout the M2 phase have been observed on the western slopes of the island (McManus et al., 2008; Sevadjian, 2008; Sevadjian et al.,

2010, 2012). In both Mamala Bay and west Oahu waters, these cold pulses were more consistent at 40–46 m but sometimes propagated to depths as shallow as 10–20 m (Sevadjian et al., 2012). The cold water intrusions at tidal frequencies observed in this study are consistent with previous observations.

Turbidity did not have strong spectral peaks at the M2/M4 frequencies, and all other parameters exhibited variability in addition to the primary scales of M2/M4. Internal solitary waves (ISWs) may be generated due to tidal processes but would not necessarily propagate and arrive at a location at tidal frequencies (Shastna and Peltier, 2005). ISWs have been shown to cause mixing and sediment resuspension while propagating close to the benthos (Bogucki et al., 1997) and could potentially contribute to the nontidal phase variability in turbidity and background variability in other parameters.

Detection of a Pollutant Nitrate Signal

The Honolulu SWAC system will introduce elevated levels of nitrate and phosphate to the base of the euphotic zone. These crucial nutrients limit phytoplankton growth in the surface ocean near Hawaii (Karl et al., 2001), so monitoring of changes in nutrient levels and biomass in the water column will be especially critical when SWAC becomes operational.

Natural variability in nitrate concentrations could make detection of anthropogenic inputs of nitrate signals difficult; however, we were able to discern a nitrate signal that likely was of anthropogenic origin. On September 9, 2013, 07:45, a large molasses spill was reported in Honolulu Harbor at a site 4.42 km from the mooring. A subsurface plume of molasses exited the harbor via the channel where the bottom mooring is located, and the nitrate content of the molasses itself was found to be 2.14 mM (Robert Bidigare, University of Hawaii, *pers. comm.*, December 4, 2014). An increase in nitrate measurements at the bottom mooring at 140 m was measured several days following the first observation of the molasses spill in the harbor, which is consistent with a slow flow of the molasses plume down the Honolulu Harbor channel. The spill would have had to travel 0.056 km hr^{-1} or 1.58 cm s^{-1} to reach the site in the 3.28 days between the time the spill was reported and the beginning of the nitrate spike in the moored data (Figure 5). This flow rate is reasonable for cross-shelf exchange.

During the spike in nitrate in mid-September 2013, the typical tidal-frequency variability continued as baseline levels of nitrate rose for several days, and then returned to normal. The observed increase in nitrate could be a direct signal from a diluted plume of molasses that flowed out of the harbor and downslope following the spill. The detection of this pollution event raises confidence in the ability of optical oceanographic equipment to detect increases in nitrate concentrations due to inputs such as those associated with SWAC operation.

SWAC Plume

Plume Water Characteristics and Potential for Enhancing Primary Production

The SWAC plume will have higher nutrient levels and lower oxygen levels than ambient conditions, and the higher nutrient levels in particular may be available to primary producers. In total, 2.91×10^6 mol yr^{-1} of nitrate will be introduced into the photic zone. For comparison, the current introduced nitrate load from sewage treatment plants is 5.7×10^5 mol yr^{-1} (Laws et al., 1999). The observed tidal-frequency changes in nutrient concentration are due to advection of denser fluid up and down the slope, which results in nitrate concentrations that vary an average of 4.6 µmol kg^{-1} throughout the day, compared to a difference of 28.6 µmol kg^{-1} between effluent water and average ambient concentrations. Other sources of nutrients are less well described; the nutrient load from stream input is unknown because most streams enter the bay through an estuary system that acts as a buffer zone, trapping most of the carbon and nutrients before they can enter the ocean ecosystem (Laws et al., 1999).

Previous studies have addressed the environmental impacts of the sewage plumes entering Mamala Bay, and they found that nutrient concentrations and particle loads were higher inside the plume, and that phytoplankton growth was stimulated under physical forcing conditions where the time scale of dilution was longer than the phytoplankton growth response (Petrenko et al., 1997). Other studies have also found significant chlorophyll *a* increases downcurrent of the sewage treatment plants (Laws et al.,

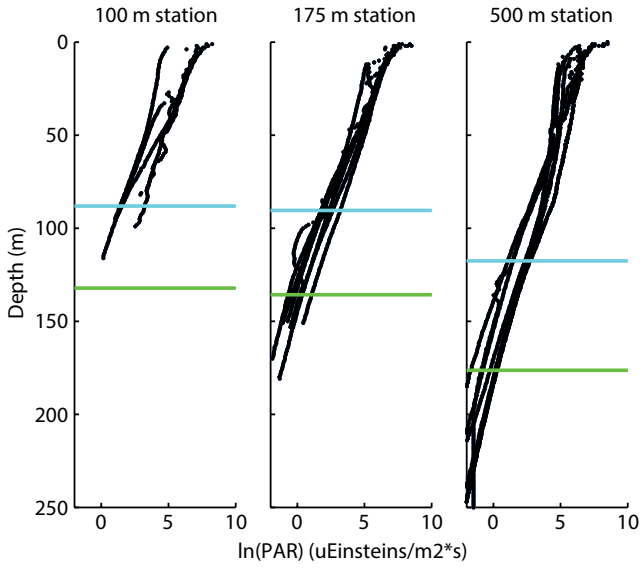


FIGURE 7. Irradiance profiles from the three profiling stations show that the 1% and 0.1% light levels are deepest at the 500 m depth station. The SWAC diffuser is located at 100–140 m depth, generally between the 1% and 0.1% light level. If the plume flows along isopycnals to deeper water, it will encounter higher light levels, increasing the possibility of SWAC-driven increases in primary productivity.

1999). These sewage plumes have bioavailable nutrients, but not in the typical ratio found in the ocean. In the case of the SWAC plume, phytoplankton are adapted to the natural nutrient ratios that will be found therein, which could increase the efficiency of their use of the nutrients.

In addition to the presence of bioavailable nutrients, the ability of primary producers to grow will depend on the residence time of the plume in depths with appropriate PAR levels. The 100–140 m range is slightly below the chlorophyll maximum, but still within the zone of adequate light to support primary production (Figure 6d). Therefore, it is possible that injection of high-nutrient water to these depths will support new primary productivity, with unknown consequences.

Advection and Diffusion of the Plume

The advection and diffusion of the plume is of critical importance to how the phytoplankton community will respond. Studies of a buoyant sewage treatment plume dilution in Mamala Bay showed that the plume generally remained trapped below 40 m, but had a complex structure, including variable shapes and patchiness that was probably driven by variations in physical conditions such as current speed, shear, water column stratification, and internal tides (Petrenko et al., 1998). Similar complexity can be expected in this sinking plume.

The plume will be denser than ambient water by approximately 2.0 kg m^{-3} (Honolulu SWAC, LLC, 2014). Buoyancy calculations indicate that the plume will tend to sink after passing through the diffuser, as the buoyancy term in the momentum balance is orders of magnitude larger than the other terms, including the bed stress. Therefore, the observed cross-shore currents are not strong enough to advect the plume back upslope. As the plume sinks downslope, it will likely continue to diffuse and entrain ambient water. Once it reaches an ambient isopycnal or range of isopycnals, the plume is expected to detach from the slope, perhaps via gravitational collapse following mixing as the plume encounters these isopycnal surfaces (McPhee-Shaw, 2006; Inall, 2009). Diffusive spreading will be important, but there is also a possibility for rapid horizontal spreading due to flow along isopycnals (Dale et al., 2006).

We are concerned that the SWAC plume is being released at a depth where the pycnocline intersects the benthos. This situation increases the potential for horizontal spreading over multiple kilometers. Regardless of the dominant spreading mechanism (flow along isopycnals or diffusive spreading), phytoplankton increases are expected if elevated levels of nutrients remain above the compensation depth.

CONCLUSIONS: RECOMMENDATIONS FOR MONITORING

The operation of a district-scale SWAC system in Honolulu, HI, will have unique environmental impacts due to the relocation of deep seawater to the base of the euphotic zone. This input of deep seawater will likely alter the environmental properties of coastal waters in the area of impact and could potentially lead to increases in phytoplankton growth and net primary production over significant horizontal scales. Given the amount of nutrients being upwelled to the photic zone, the variety of physical factors that may influence the SWAC plume's shape in Mamala Bay, and the observations of increased chlorophyll *a* in the treated sewage plumes, we recommend expanding the environmental monitoring program during SWAC operation. The operational monitoring plan must be well resolved temporally and spatially because the way the plume will spread is not understood and is likely to be variable according to changing physical conditions (Petrenko et al., 1998). An increase in nutrient concentrations above the compensation depth will likely result in changes in primary production rates and ultimately in plankton biomass.

Other environmental impacts related to SWAC operations have not been discussed thoroughly here, but we must be aware of other effects such as introduction of microbial species from depth, attraction or avoidance of nekton (NOAA, 2010; Comfort and Vega, 2011), and effects related to high nitrous oxide concentrations, low pH, and high CO_2 in the effluent water. Overall, there are likely to be some measurable environmental impacts from SWAC operations. The plume is not expected to surface, and the plumes from wastewater treatment facilities have not been found to impact shoreline water quality, which is very important for Honolulu's tourism-based economy. Nevertheless, we must be conscious of the possible additive impacts of releasing more nutrient-rich water into the ecosystem, in quantities that would increase water input to the bay by 20–35%.

SUPPLEMENTARY MATERIALS. Specifics of moored and profiling instruments and programming are available online at http://www.tos.org/oceanography/archive/28-2_comfort.html.

ACKNOWLEDGEMENTS. Funding for this work was provided by the Office of Naval Research, the State of Hawaii, the National Science Foundation (C-MORE; EF04-24599), and the Gordon and Betty Moore Foundation. We would also like to thank the following people for field and shore-based assistance: Sarah Searson, Tara Clemente, Lance Fujieki, Rebecca Briggs, Gordon Walker, and Carly Quisenberry. Finally, we thank the University of Hawaii Marine Center, Parker Marine Corp., and Sea Engineering Inc. for vessel support.

REFERENCES

Alford, M.H., M.C. Gregg, and M.A. Merrifield. 2006. Structure, propagation, and mixing of energetic baroclinic tides in Mamala Bay, Oahu, Hawaii. *Journal of Physical Oceanography* 36:997–1,018, http://dx.doi.org/10.1175/JPO2877.1.

Arent, D.J., A. Wise, and R. Gelman. 2011. The status and prospects of renewable energy for combating global warming. *Energy Economics* 33:584–593, http://dx.doi.org/10.1016/j.eneco.2010.11.003.

Baines, P.G. 2001. Mixing in flows down gentle slopes into stratified environments. *Journal of Fluid Mechanics* 443:237–270, http://dx.doi.org/10.1017/S0022112001005250.

Boehlert, G.W., and A.B. Gill. 2010. Environmental and ecological effects of ocean renewable energy development: A current synthesis. *Oceanography* 23(2):68–81, http://dx.doi.org/10.5670/oceanog.2010.46.

Brillinger, D.R. 2002. John W. Tukey's work on time series and spectrum analysis. *Annals of Statistics* 30:1,595–1,618, http://dx.doi.org/10.1214/aos/1043351248.

Bogucki, D., T. Dickey, and L.G. Redekopp. 1997. Sediment resuspension and mixing by resonantly generated internal solitary waves. *Journal of Physical Oceanography* 27:1,181–1,196, http://dx.doi.org/10.1175/1520-0485(1997)027<1181:SRAMBR>2.0.CO;2.

Bondur, V.G., N.N. Filatov, Y.V. Grebenyuk, Y.S. Dolotov, R.E. Zdorovennov, M.P. Petrov, and M.N. Tsidilina. 2007. Studies of hydrophysical processes during monitoring of the anthropogenic impact on coastal basins using the example of Mamala Bay of Oahu Island in Hawaii. *Oceanology* 47:769–787, http://dx.doi.org/10.1134/S0001437007060033.

Comfort, C.M., and L. Vega. 2011. Environmental assessment for ocean thermal energy conversion in Hawaii: Available data and a protocol for baseline monitoring. In *Proceedings of the Oceans'11 MTS/IEEE Kona Conference*, September 19–22, 2011. Institute of Electrical and Electronics Engineers, Piscataway, NJ, 8 pp.

Cooley, J.W., and J.W. Tukey. 1965. An algorithm for the machine calculation of complex Fourier series. *Mathematics of Computation* 19:297–301, http://dx.doi.org/10.1090/S0025-5718-1965-0178586-1.

Dale, A.C., M.D. Levine, J.A. Barth, and J.A. Austin. 2006. A dye tracer reveals cross-shelf dispersion and interleaving on the Oregon shelf. *Geophysical Research Letters* 33, L03604, http://dx.doi.org/10.1029/2005GL024959.

Eich, M.L., M.A. Merrifield, and M.H. Alford. 2004. Structure and variability of semidiurnal internal tides in Mamala Bay, Hawaii. *Journal of Geophysical Research* 109, C05010, http://dx.doi.org/10.1029/2003JC002049.

Freeman, W. 1993. *Revised Total Maximum Daily Load Estimates for Six Water Quality Limited Segments, Island of Oahu, Hawaii*. Report prepared for the State of Hawaii Department of Health Environmental Planning Office, Honolulu, HI.

Gill, A.B. 2005. Offshore renewable energy: Ecological implications of generating electricity in the coastal zone. *Journal of Applied Ecology* 42:605–615, http://dx.doi.org/10.1111/j.1365-2664.2005.01060.x.

Harrison, J. 1987. *The 40 MWe OTEC Plant at Kahe Point, Oahu, Hawaii: A Case Study of Potential Biological Impacts*. National Oceanic and Atmospheric Administration, National Marine Fisheries Service, Southwest Fisheries Center, Honolulu, HI, NOAA-TM-MNFS-SWFC-68, 105 pp., http://www.pifsc.noaa.gov/tech/NOAA_Tech_Memo_068.pdf.

Hayward, T.L. 1987. The nutrient distribution and primary production in the central North Pacific. *Deep Sea Research Part A* 34(9):1,593–1,627, http://dx.doi.org/10.1016/0198-0149(87)90111-7.

Honolulu SWAC (Seawater Air Conditioning), LLC. 2014. *Final Environmental Impact Statement for the Proposed Honolulu Seawater Air Conditioning Project, Honolulu, Hawai'i.* Prepared by Cardno TEC, Inc., United States Army Corps of Engineers, Honolulu, HI, 834 pp.

Inall, M.E. 2009. Internal wave induced dispersion and mixing on a sloping boundary. *Geophysical Research Letters* 36, L05604, http://dx.doi.org/10.1029/2008GL036849.

Ivanov, V.V., G.I. Shapiro, J.M. Huthnance, D.L. Aleynik, and P.N. Golovin. 2004. Cascades of dense water around the world ocean. *Progress in Oceanography* 60:47–98, http://dx.doi.org/10.1016/j.pocean.2003.12.002.

Karl, D.M. 2014. The contemporary challenge of the sea: Science, society, and sustainability. *Oceanography* 27(2):208–225, http://dx.doi.org/10.5670/oceanog.2014.57.

Karl, D.M., K.M. Björkman, J.E. Dore, L. Fujieki, D.V. Hebel, T. Houlihan, R.M. Letelier, and L.M. Tupas. 2001. Ecological nitrogen-to-phosphorus stoichiometry at station ALOHA. *Deep Sea Research Part II* 48:1,529–1,566, http://dx.doi.org/10.1016/S0967-0645(00)00152-1.

Kirk, J.T.O. 1994. *Light and Photosynthesis in Aquatic Ecosystems*, 2nd ed. Cambridge University Press, New York, NY, 509 pp.

Laws, E.A., R.M. Letelier, and D.M. Karl. 2014. Estimating the compensation irradiance in the ocean: The importance of accounting for non-photosynthetic uptake of inorganic carbon. *Deep Sea Research Part I* 93:35–40, http://dx.doi.org/10.1016/j.dsr.2014.07.011.

Laws, E.A., D. Ziemann, and D. Schulman. 1999. Coastal water quality in Hawaii: The importance of buffer zones and dilution. *Marine Environmental Research* 48:1–21, http://dx.doi.org/10.1016/S0141-1136(99)00029-X.

Leichter, J.J., H.L. Stewart, and S.L. Miller. 2003. Episodic nutrient transport to Florida coral reefs. *Limnology and Oceanography* 48:1,394–1,407, http://dx.doi.org/10.4319/lo.2003.48.4.1394.

Levitus, S. 1982. *Climatological Atlas of the World Ocean*. National Oceanic and Atmospheric Association Professional Paper 13. US Government Printing Office, Washington, DC, 173 pp.

Lilley, J., D. Konan, D. Lerner, and D. Karl. 2012. *Potential Benefits, Impacts, and Public Opinion of Seawater Air Conditioning in Waikiki*. Center for Sustainable Coastal Tourism. Honolulu, HI, 9 pp.

Martini, K.I., M.H. Alford, J.D. Nash, E. Kunze, and M.A. Merrifield. 2007. Diagnosing a partly standing internal wave in Mamala Bay, Oahu. *Geophysical Research Letters* 34, L17604, http://dx.doi.org/10.1029/2007GL029749.

McManus, M.A., K.J. Benoit-Bird, and C.B. Woodson. 2008. Behavior exceeds physical forcing in the diel horizontal migration of a midwater sound-scattering layer in Hawaiian waters. *Marine Ecology Progress Series* 365:91–101, http://dx.doi.org/10.3354/meps07491.

McPhee-Shaw, E. 2006. Boundary–interior exchange: Reviewing the idea that internal-wave mixing enhances lateral dispersal near continental margins. *Deep Sea Research Part II* 53:42–59, http://dx.doi.org/10.1016/j.dsr2.2005.10.018.

Merrifield, M.A., P.E. Holloway, and T.M. Johnston. 2001. The generation of internal tides at the Hawaiian Ridge. *Geophysical Research Letters* 28:559–562, http://dx.doi.org/10.1029/2000GL011749.

Myers, E.P., D. Hoss, W. Matsumoto, D. Peters, M. Seki, R. Uchida, J. Ditmars, and R. Paddock. 1986. *The Potential Impact of Ocean Thermal Energy Conversion (OTEC) on Fisheries*. NOAA Technical Report NMFS 40, US Department of Commerce, National Oceanic and Atmospheric Administration, National Marine Fisheries Service, Washington, DC, 39 pp., http://spo.nwr.noaa.gov/tr40opt.pdf.

Nash, J.D., E. Kunze, C. Lee, and T. Sanford. 2006. Structure of the baroclinic tide generated at Kaena Ridge, Hawaii. *Journal of Physical Oceanography* 36:1,123–1,135, http://dx.doi.org/10.1175/JPO2883.1.

NOAA (National Oceanic and Atmospheric Administration). 1981. *Ocean Thermal Energy Conversion Cinal Environmental Impact Statement.* United States Department of Commerce, National Oceanic and Atmospheric Administration, Office of Ocean Minerals and Energy, Charleston, SC, 284 pp., http://coastalmanagement.noaa.gov/programs/media/otec1981feis.pdf.

NOAA. 2010. *Ocean Thermal Energy Conversion: Assessing Potential Physical, Chemical, and Biological Impacts and Risks*. Prepared by Coastal Response Research Center, University of New Hampshire, Durham, NH, 39 pp., http://coast.noaa.gov/czm/media/otecjun10wkshp.pdf.

Pelc, R., and R. Fujita. 2002. Renewable energy from the ocean. *Marine Policy* 26:471–479, http://dx.doi.org/10.1016/S0308-597X(02)00045-3.

Petrenko, A.A., B.H. Jones, and T.D. Dickey. 1998. Shape and initial dilution of Sand Island, Hawaii sewage plume. *Journal of Hydraulic Engineering* 124:565–571, http://dx.doi.org/10.1061/(ASCE)0733-9429(1998)124:6(565).

Petrenko, A.A., B.H. Jones, T.D. Dickey, and P. Hamilton. 2000. Internal tide effects on a sewage plume at Sand Island, Hawaii. *Continental Shelf Research* 20:1–13, http://dx.doi.org/10.1016/S0278-4343(99)00060-6.

Petrenko, A.A., B.A. Jones, T.D. Dickey, M. LeHaitre, and C. Moore. 1997. Effects of a sewage plume on the biology, optical characteristics, and particle size distributions of coastal waters. *Journal of Geophysical Research* 102(C11):25,061–25,071, http://dx.doi.org/10.1029/97JC02082.

Sevadjian, J.C. 2008. The effects of physical structure and processes on thin zooplankton layers in Mamala Bay, Hawaii. MS thesis, University of Hawaii at Manoa, HI.

Sevadjian, J.C., M.A. McManus, K.J. Benoit-Bird, and K.E. Selph. 2012. Shoreward advection of phytoplankton and vertical re-distribution of zooplankton by episodic near-bottom water pulses on an insular shelf: Oahu, Hawaii. *Continental Shelf Research* 50:1–15, http://dx.doi.org/10.1016/j.csr.2012.09.006.

Sevadjian, J.C., M.A. McManus, and G. Pawlak. 2010. Effects of physical structure and processes on thin zooplankton layers in Mamala Bay, Hawaii. *Marine Ecology Progress Series* 409:95–106, http://dx.doi.org/10.3354/meps08614.

Shastna, M., and W.R. Peltier. 2005. On the resonant generation of large-amplitude internal solitary and solitary-like waves. *Journal of Fluid Mechanics* 543:267–292, http://dx.doi.org/10.1017/S002211200500652X.

Stevenson, M., J. O'Connor, and J. Aldrich. 1996. *Mamala Bay Study: Pollutant Source Identification*. Mamala Bay Study Commission, Pacific Islands Ocean Observing System, MB-3, Honolulu, HI, 83 pp.

War, J.C. 2011. Seawater Air Conditioning (SWAC): A renewable energy alternative. In *Proceedings of the Oceans'11 MTS/IEEE Kona Conference*, September 19–22, 2011. Institute of Electrical and Electronics Engineers, Piscataway, NJ, 9 pp.

AUTHORS. **Christina M. Comfort** (ccomfort@hawaii.edu) is Oceanographic Research Specialist, Department of Oceanography, School of Ocean and Earth Science and Technology (SOEST), University of Hawaii, Honolulu, HI, USA. **Margaret A. McManus** is Professor, Department of Oceanography, SOEST, University of Hawaii, Honolulu, HI, USA. **S. Jeanette Clark** is Oceanographer, Joint Institute for Marine and Atmospheric Research, University of Hawaii, Honolulu, HI, USA. **David M. Karl** is Victor and Peggy Brandstrom Pavel Chair in Ocean Science and Professor of Oceanography, University of Hawaii at Manoa, and Daniel K. Inouye Center for Microbial Oceanography: Research and Education, Honolulu, HI, USA. **Chris E. Ostrander** is Assistant Dean, SOEST, University of Hawaii, Honolulu, HI, USA.

ARTICLE CITATION

Comfort, C.M., M.A. McManus, S.J. Clark, D.M. Karl, and C.E. Ostrander. 2015. Environmental properties of coastal waters in Mamala Bay, Oahu, Hawaii, at the future site of a seawater air conditioning outfall. *Oceanography* 28(2):230–239, http://dx.doi.org/10.5670/oceanog.2015.46.